

# A Semi-Active Robot for Steep Obstacle Ascent

S Avinash , V V Anurag , A K Singh , S V Shah , K M Krishna

**Abstract**—In this paper we propose a semi-active robot for climbing steep obstacles like steps, curbs, etc. The key novelty of the proposed robot lies in the use of a passive mechanism for climbing steps of smaller heights and motor only while climbing steps of bigger heights. Analysis of the robot's stability during its ascent phase is also investigated. Model based control is used to achieve step climbing. The other novelty of the robot, in contrast to existing active suspension step climbers, is that it does not need the knowledge of step height beforehand. Therefore, the mechanism has the advantage of height-independent climbing motion as in the case of passive mechanism along with the extra freedom of active joints for maintaining vehicle stability, only when required. Efficacy of the mechanism is exhibited through simulations on steps of various heights.

## I. INTRODUCTION

The last decade has seen a surge of interest in the potential applications of robots in urban search and rescue missions [1]. The use of robots for rescue missions and surveillance would help to curtail human loss and augment rescue efforts. Given such scenarios, one would expect the robot to navigate over highly uneven surfaces autonomously with little or no help from the surroundings. Particularly, in urban scenarios, robots designed to traverse over structured obstacles (such as steps) with good terrainability [8], would have a distinct edge. This paper proposes a novel mechanism to serve this purpose.

Research into design of rough terrain vehicles has broadly led to two classes of vehicles: active suspension and passive suspension. The elegance of passive suspension vehicles [2], [7], [6] lies in their ability to surmount steep obstacles by the virtue of only wheel-ground contact forces with the help of appropriately designed linkages. This greatly simplifies the control architecture of the vehicle. But their climbing ability is limited to obstacles whose height is upto twice their wheel diameters [2]. On the other hand, active suspension mechanisms [3], [5], [9], [4] have simplified kinematic architecture but may require complicated control algorithms to maintain stability while climbing. In [5], it was shown that the shifting the Centre-of-Mass(COM) upwards while climbing(using actuators) enabled the robot to climb higher obstacles than its passive suspension counterparts. Similarly, in [9], posture controller was implemented during step climbing. However, the climbing ability of the active suspension robots is limited to heights upto 1.5 times the length of an individual link in the robot.

It is ideal to have a mechanism which has compliance offered by the passive systems and an optimal number of actuators to enforce a control scheme for climbing higher steps. The mechanism must be able to climb steps of lower

heights using only wheel actuation with the help of compliance. The use actuators will be limited to climbing bigger steps only. Such a scheme must be able to achieve height-independent climbing motion [5] also. This motivated us to propose a mechanism which satisfies the above requirements.

In Section II, the proposed mechanism is described. The control methodology used to maintain stability while climbing is detailed in Section III. In Section IV, the simulation results are discussed and finally the conclusions are given in Section V.

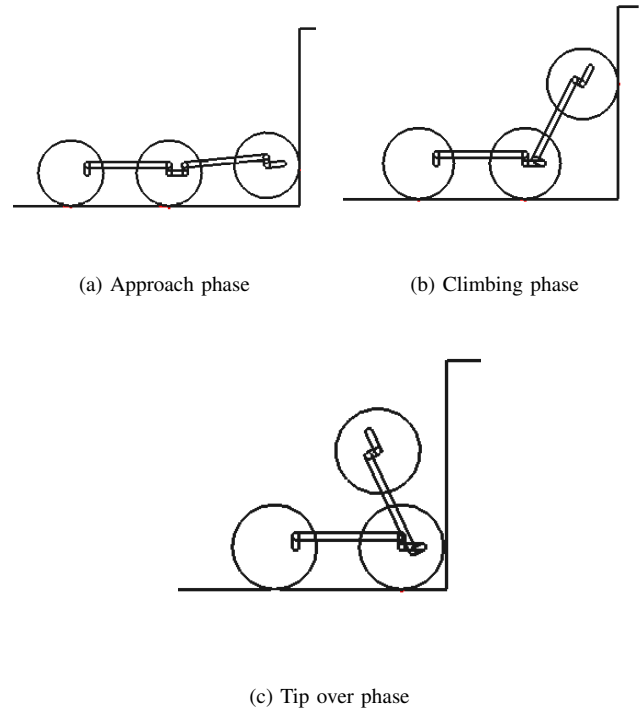


Fig. 1. a)-c) A fully passive mechanism climbing a step whose height is greater than the individual link length

## II. MODEL DESCRIPTION

The proposed mechanism evolves from a 2-linked passive suspension vehicle shown in Figs. 1(a)-1(c). This vehicle consists of two rigid links with wheels, connected to each other through a revolute joint.

The free body diagram for this two link system is shown in the Fig. 2. It can be seen that once the first wheel comes in contact with the obstacle, a horizontal normal force  $N_1$  and the resulting traction force  $F_1$  are generated. The moments generated by these two forces are responsible for lifting link

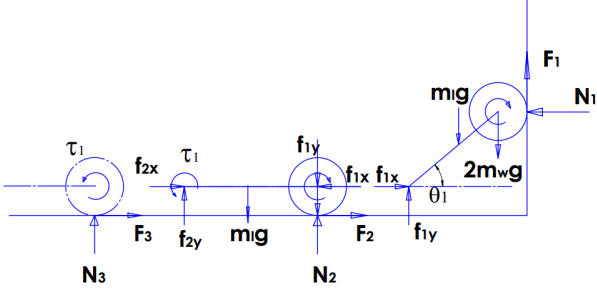


Fig. 2. Free body diagram of the 2-linked system

1 off the ground and climbing the obstacle. Static equilibrium equations of the system under study are shown below.

$$N_1 = F_2 + f_{2x} \quad (1)$$

$$N_2 = 2mg - F_1 + f_{2y} \quad (2)$$

$$F_1 l \cos \theta_1 + N_1 l \sin \theta_1 - 2m_w g l \cos \theta_1 - m_l g (l/2) \cos \theta_1 = 0 \quad (3)$$

Here,  $f_{ix}$  and  $f_{iy}$  represent the reaction forces at joint  $i$  in  $x$  and  $y$  directions, respectively. Similarly,  $F_i$  denotes the traction force generated by the  $i^{th}$  wheel.  $m$  denotes the total mass of link and wheel module, i.e.  $2m_w + m_l$ , where  $m_w$  and  $m_l$  denote the masses of wheel and link, respectively. The counter clockwise moments (about link joint  $L_1$ ) responsible for lifting link 1 come from  $N_1$  and  $F_1$ , as evident from (3). Moreover,  $F_1 \leq \mu N_1$ , where  $\mu$  is the coefficient of friction. The only clockwise moment, resisting the lift, is due to the self weight of the link. Hence, it is desirable to have lighter links and a higher  $N_1$ . Note that, in general  $N_1 = \sum_{i=2}^n F_i$ . This can be derived from equation (1) where  $f_{2x}$  is equal to the sum of the traction forces ( $F_i$ 's) of all the wheels connected to trailing joints. The passive mechanism is able to climb steps purely based on this push force ( $N_1$ ). Since it is a modular system, one can always add or subtract links depending on the push force required and coefficient of friction ( $\mu$ ) of the given terrain. The mechanism proposed here uses 5 links.

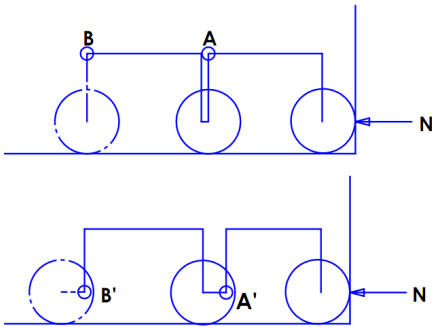


Fig. 3. Two potential joint positions

Another important design aspect to be considered is the placement of the link joint. It is desirable to profitably use

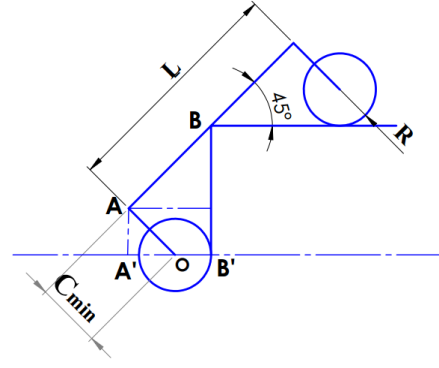


Fig. 4. Configuration used for  $C_{min}$  calculation

$N_1$  in lifting the first link by generating a counter clockwise moment when the wheel is pressed against the obstacle. Note the first configuration shown in Fig. 3. In this case, when the link joint is placed above the line joining the wheel axes,  $N_1$  will create a clockwise moment about that link joint and resists the link from lifting up. A high value of  $N_1$  may even cause link 1 to fold inwards, which is undesirable. Therefore, the joint must lie on or below that line which joins wheel centres. In the proposed mechanism, the joint is on that line, as shown by the second configuration in Fig. 3. When the wheel collides with the obstacle, the moment due to  $N_1$  is zero about the joint. The counter clockwise moment due to  $F_1$  will initially help in lifting the wheel off the ground. Thereafter, the counter clockwise moment due to  $N_1$  will gradually increase helping in the link's ascent.

A minimum clearance,  $C_{min}$ , is required to ensure that none of the robot's links hit obstacles blunter than a step.  $C_{min}$  is calculated from equation (4) which is derived based on the configuration shown in Fig. 4.

$$C_{min} = l/2 - \sqrt{2}r \quad (4)$$

This passive mechanism is successfully able to climb heights less than one link length (Figs. 7(a)-7(d)). However, if the height of the step is greater than the length of the link, the first link tips over as shown in Figure 1(c). It can be inferred that if the first link crosses a certain angle, it will tip over because of the moment due to gravity. This tip over angle is  $\theta_{to} = \pi/2 - \tan^{-1}(\frac{y_{cm}}{x_{cm}})$  where  $x_{cm}$  and  $y_{cm}$  are the coordinates of the center of mass of the link-wheel module from the joint. Noting this drawback, use of an active joint at  $L_2$  is proposed. By lifting the succeeding link at an appropriate time, one can control the angle of the leading link and help it climb higher without violating the above condition. This forms the basis for this work.

Figures 5 and 6 show the isometric and front views of the proposed mechanism. It consists of two passive suspension mechanisms (as in Fig. 1(a)) connected in series. The wheel joints and link joints are denoted by  $W_1 - W_6$  and  $L_1 - L_4$ , respectively. The detailed specifications of the robot are given in Table I.

## SPECIFICATIONS OF THE ROBOT

Symbols	Quantity	Values(with Units)
$l$	Link Length	0.18 $m$
$b$	Link Breadth	0.15 $m$
$r$	Wheel Radius	0.06 $m$
$l_0$	Wheel Joint and Link Joint Offset	0.03 $m$
$\mu$	Coefficient of Friction	0.8
$\tau_{lmax}$	Max Torque of Link Motors	15 $Nm$
$\tau_{wmax}$	Max Torque of Wheel Motors	4 $Nm$
$m_w$	Mass of Each Wheel	0.5 $Kg$
$m_l$	Mass of Each Link	0.5 $Kg$
$I_w$	Moment of Inertia of the Wheel	0.000467 $Kgm^2$
$I_l$	Moment of Inertia of the Links	0.002049 $Kgm^2$

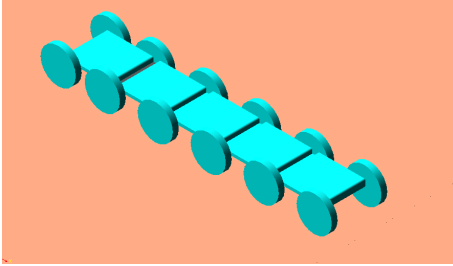


Fig. 5. Isometric view of the robot

In the next section, we discuss how one can avoid tip over during climbing using an appropriate control algorithm.

### III. CONTROL STRATEGIES

The control algorithm is designed to maintain  $\theta < \theta_{to}$  throughout the ascent. Here,  $\theta_i$  is defined as the angle between the  $i^{th}$  link and the ground. The angle  $\theta_i$  can also be defined in terms of relative joint angle  $\phi_i$  (between links  $i$  and  $i + 1$ ) as,

$$\theta_i = \sum_i^n \phi_i \quad (5)$$

Noting that the mechanism shown in figure fails when  $\theta \geq \theta_{to}$ , it can be deduced that a control over the relative joint angles  $\phi_i$  between the links can help in climbing greater heights before  $\theta_1$  approaches  $\theta_{to}$ .

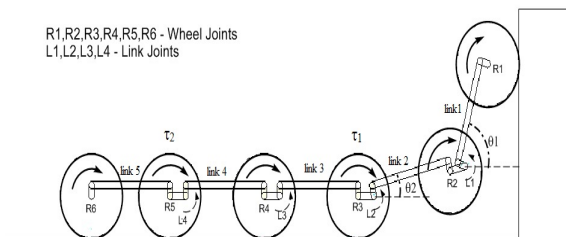


Fig. 6. Link and wheel joint nomenclature

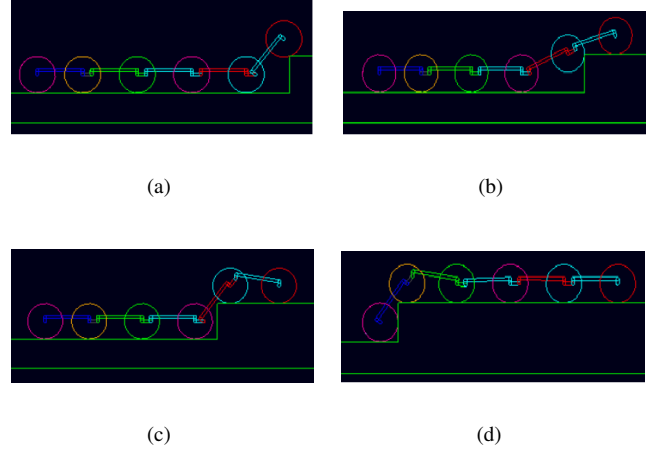


Fig. 7. Snapshots of a fully passive system climbing a step of 120 mm

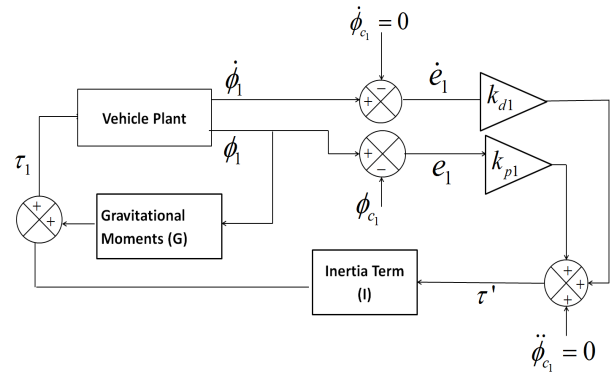


Fig. 8. Model Based Control for controlling Link 1

### A. Control Strategy I

This strategy uses only one active joint (which is at  $L2$ ) for maintaining vehicle stability. When only link 1 is climbing the step and link joint  $L2$  is actuated, two effects are seen, 1) link 1 is lifted up and 2)  $\theta_1$  is reduced. Therefore, the robot is able to climb higher steps, which could not have been possible with passive joints. To implement this control algorithm on the vehicle, a control law is developed. It is worth noting when  $\theta \ll \theta_{to}$ , the robot can climb without any actuation at the link joints. Thus, energy is conserved by minimizing the actuation of joint  $L2$  by setting up a threshold value. Hence, we define  $\phi_c = \theta_{to} - 15^\circ$ , the threshold angle, below which the robot works as a passive mechanism.

For the system under study,  $\theta_{to} = 75^0$  and hence  $\phi_c = 60^0$ . Let an error  $e_i$  be defined for the  $i^{th}$  joint angle as

$$e_i = \phi_i - \phi_c \quad (6)$$

With the above definition, a control system is designed the block diagram of which is shown in Fig. 8.

When the error obtained from (6) is greater than zero, the actuator at  $L2$  is activated. The torque actuation of the motors can be written as

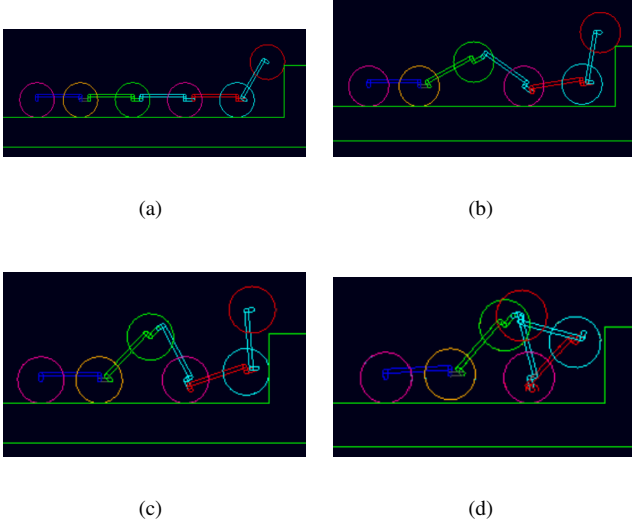


Fig. 9. Snapshots of a system failing to climb a step of 180 mm using only Strategy I

$$\tau_1 = \alpha \tau'_1 + \beta \quad (7)$$

$$\tau'_1 = \ddot{\phi}_{c1} + k_{p1}e_1 + k_{d1}\dot{e}_1 \quad (8)$$

In (8),  $k_{p1}$  and  $k_{d1}$  are proportional and derivative gains of the control system. In (7),  $\alpha$  is the inertia of links 1 and 2 about joint  $L2$ .  $\beta$  balances the moments generated due to gravity.

It is worth noting that when robot starts climbing, its 1<sup>st</sup> and 2<sup>nd</sup> links lift up in the beginning. The model based control of those two links is carried out by assuming them to be a 2-link robotic system. Other links are not controlled as they assumed to be on the ground.

The simulation results are shown in Figs. 9(a)-9(d). As stated earlier, motors are actuated to control joint angles between the links only when a certain threshold ( $\phi_c$ ) is crossed. Figure 9(c) depicts that as the second wheel is being lifted, the reaction moment generated at  $L3$  lifts link 3 off the ground. As both links 3 and 2 are being lifted, the angular displacement of link 2 with respect to the ground (i.e.,  $\theta_1$ ) may not be enough for successful climbing motion. As a result the mechanism failed to climb the step. Implementation of a similar strategy on joint  $L4$  cannot solve this problem as the error term will always be negative.

### B. Control Strategy II

This strategy uses two active joints at  $L2$  and  $L4$  for maintaining stability while climbing steps. Here, joint  $L2$  is controlled using strategy illustrated in the previous subsection while joint  $L4$  is controlled using PD control law. It is necessary to balance the reaction moment generated while actuating joint  $L2$  as detailed in Control Strategy-I. In this strategy, an extra motor is used at link joint  $L4$  for this purpose. A PD control scheme is used to counter the reactive

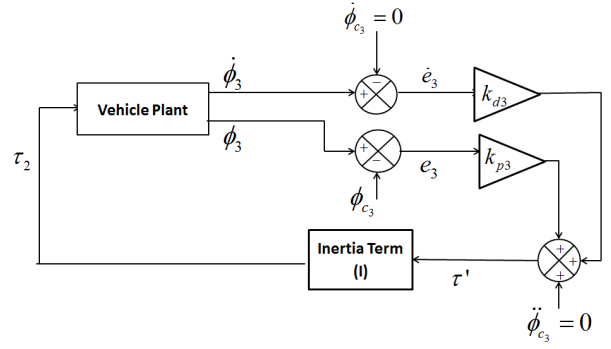


Fig. 10. PD Control for countering the reactive moment

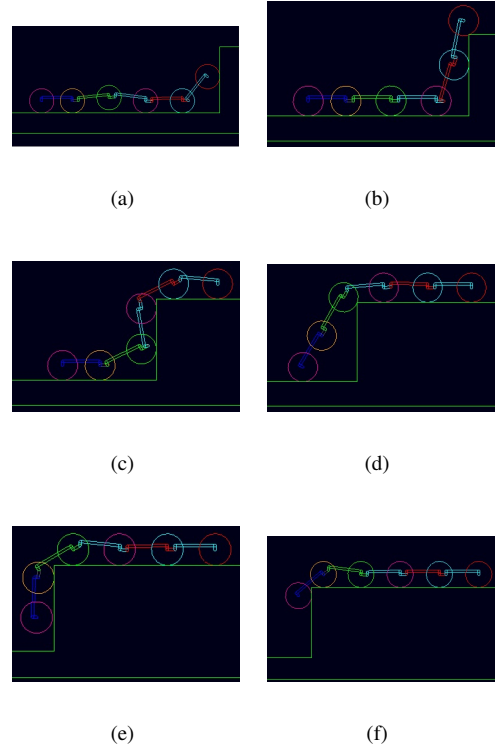


Fig. 11. Snapshots of the robot climbing a step of height 330mm using Control Strategy II

moment acting on link 3. This is actuated only when  $\phi_3 < 0$  and joint  $L2$  is active. The PD control law ensures that active joint  $L2$  only lifts link 2 while it keeps link 3 grounded. The control architecture for the same is shown in the Fig. 10.

It is worth noting that the actuation of  $L4$  might lift off the fifth wheel when the reaction moment to be balanced is high. In order to overcome this disadvantage, a torsional spring is fitted at the passive joint  $L3$ . One cannot choose a spring of high stiffness as this makes the joint stiff. this may limit the climbing ability of the vehicle. After carefully considering the above aspects, a torsional spring of stiffness 2 Nm/rad is chosen. Figures 11(a)-11(f) show that the mechanism was successfully able to climb a step of height 330 mm using the proposed strategy.

#### IV. RESULTS

The robot was simulated in the MSC ADAMS software's dynamics simulation environment to study its performance on steps of varying heights. The Step height was parametrized in terms of link length. The speed of the robot is  $18 \text{ cm/s}$ . The values of  $k_{p1}$  and  $k_{d1}$  for the model based control in (8) are taken as 20 and 4, respectively. Similarly, values of  $k_{p2}$  and  $k_{d2}$  used in the PD control at link joint L4 are 80 and 10, respectively.

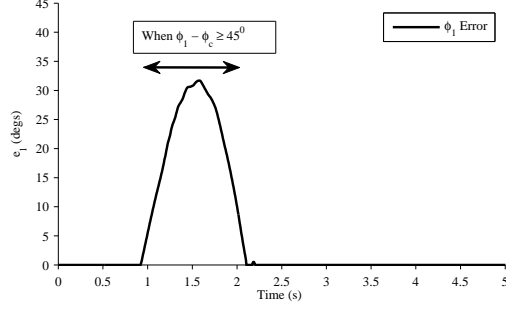


Fig. 12. Error vs Time plot

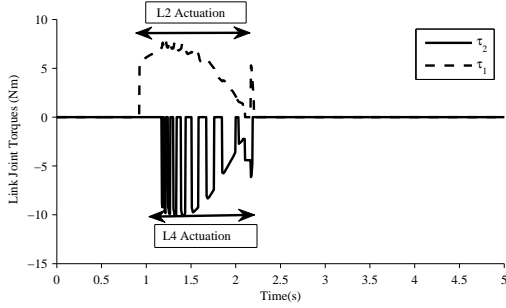


Fig. 13. Active joint torques vs Time

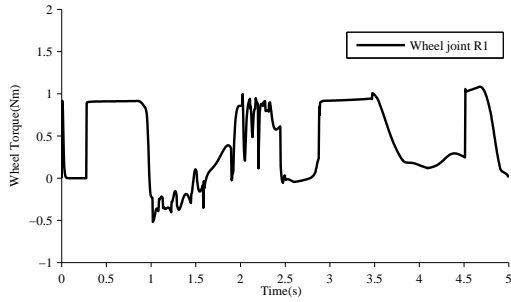


Fig. 14. Wheel torques vs Time

Fig. 13 shows the amount of torque required at the motors during ascent. It can be seen that, while ascending the first step, L4 applies nearly equal amount of torque (in the counter direction) as L2. Fig. 12 shows the plot of  $e_1$  with respect to time, calculated after the angle  $\phi_1$  reaches threshold angle,  $\phi_c = 45^\circ$ . The threshold is lowered to study the performance of the controller at a lower threshold value. The Control Strategy succeeded in ensuring that link 1 doesn't tip

over during its ascent. Thus, the robot achieves the desired climbing motion for heights upto  $330 \text{ mm}$  which is nearly 1.8 times its link length.

Simulations were also carried out on irregular terrains, as shown in Figs. 15(a)-15(g). The modularity and passivity of the robot give it a natural edge while traversing an irregular terrain. The body of the robot is able to deform itself along the shape of the obstacle and in areas where the angle of deformation is greater than  $\phi_c$ , the active joint helps it in climbing without tipping over.

#### V. CONCLUSIONS AND FUTURE WORK

In this work, a simple design of a modular semi-active step climbing robot has been presented. The novelty of the robot lies in the fact that it can climb heights upto 1.8 times of the link length. Two control strategies have been presented to achieve step climbing. In the first strategy only joint L2 was actuated when  $\theta_1 \geq \theta_c$ . This strategy showed some improvement over the passive mechanism but it failed to climb heights higher than 1.2 times the link

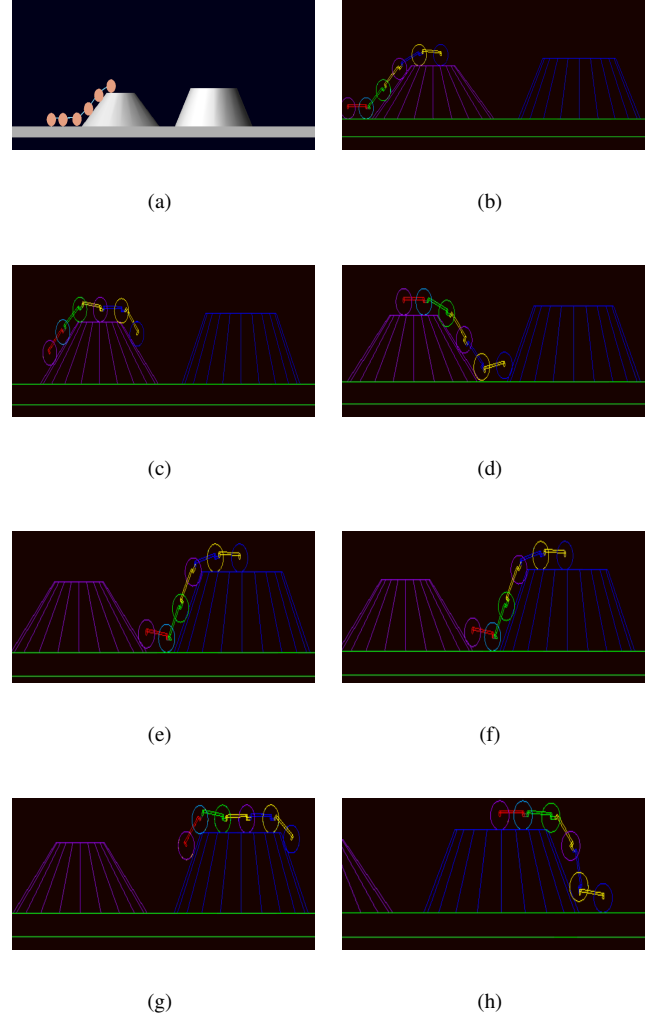


Fig. 15. Snapshots of the robot climbing steep obstacles

length. In the second strategy joints  $L2$  and  $L4$  have been actuated to overcome the above disadvantage. The robot was successfully able to climb the height equal to 1.8 times the link length.

The proposed strategy allows the robot to move passively for smaller steps and semi-actively for bigger steps. This makes this robot very desirable for traversing on an irregular terrains and step-like obstacles in an energy efficient manner. However, the robot's climbing ability is limited to heights less than  $2l\sin\theta_{to}$ .

Development of a working prototype of the proposed mechanism will be carried out as future work. Work also needs to be done on developing control schemes to achieve safe climbing down motion. Use of springs instead of motors to achieve similar performance can also be explored.

#### REFERENCES

- [1] A. Davids. Urban search and rescue robots: from tragedy to technology. *IEEE Intelligent Systems*, 17(2):81–83, 2002.
- [2] T. Estier, Y. Crausaz, B. Merminod, M. Lauria, R. Piguet, and R. Siegwart. An innovative space rover with extended climbing abilities. *Proceedings of Space and Robotics*, 2000:333–339, 2000.
- [3] C. Grand, F. BenAmar, F. Plumet, and P. Bidaud. Decoupled control of posture and trajectory of the hybrid wheel-legged robot hylos. *IEEE International Conference on Robotics and Automation (ICRA)*, 5:5111–5116, 2004.
- [4] K. Iagnemma, A. Rzepniewski, S. Dubowsky, and P. Schenker. Control of robotic vehicles with actively articulated suspensions in rough terrain. *Autonomous Robots*, 14(1):5–16, 2003.
- [5] A. Kamimura and H. Kurokawa. High-step climbing by a crawler robot dir-2-realization of automatic climbing motion. *IEEE/RSJ International Conference on Intelligent Robots and Systems (IROS)*, pages 618–624, 2009.
- [6] P. Lamon and R. Siegwart. Wheel torque control in rough terrain-modeling and simulation. *IEEE International Conference on Robotics and Automation (ICRA)*, pages 867–872, 2005.
- [7] A. Singh, R. Namdev, V. Eathakota, and K. Krishna. A novel compliant rover for rough terrain mobility. *IEEE/RSJ International Conference on Intelligent Robots and Systems (IROS)*, pages 4788–4793, 2010.
- [8] T. Thueer and R. Siegwart. Mobility evaluation of wheeled all-terrain robots. *Robotics and Autonomous Systems*, 58(5):508–519, 2010.
- [9] K. Turker, I. Sharf, and M. Trentini. Step negotiation with wheel traction: a strategy for a wheel-legged robot. *IEEE International Conference on Robotics and Automation (ICRA)*, pages 1168–1174, 2012.